Supporting Information

Ce-Doped FeNi Layered Double Hydroxide Nanosheets Grown on Open-Framework Nickel Phosphate Nanorods Array for Oxygen Evolution Reaction

Shifeng Li*, Zihao Liu, Fangfang Wang, Feifei Yuan and Yonghong Ni*

College of Chemistry and Materials Science, Key Laboratory of Functional Molecular Solids, Ministry of Education, Anhui Provincial Engineering Laboratory for New-Energy Vehicle Battery Energy-Storage Materials, Anhui Normal University, 189 Jiuhua Southern Road, Wuhu, 241002, PR China. Fax: +86-553-3869303. E-mail: sfli@mail.ahnu.edu.cn (S. F. Li) niyh@mail.ahnu.edu.cn (Y. H. Ni)

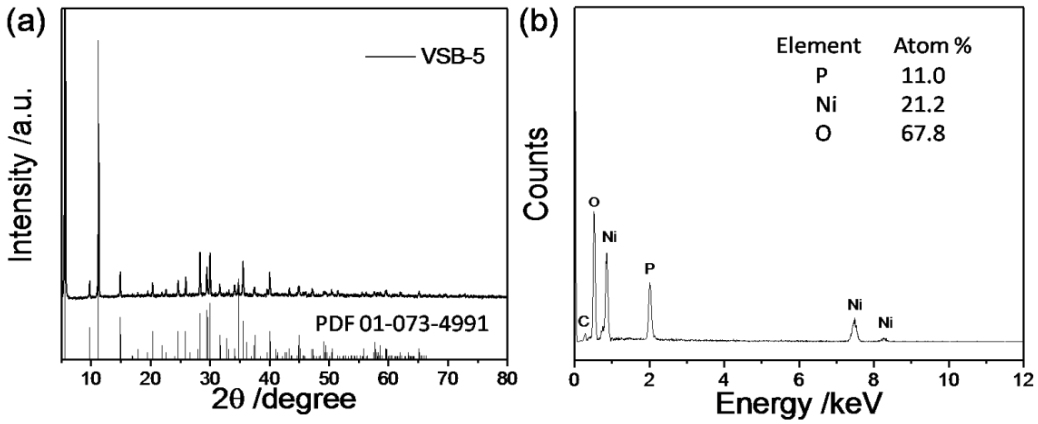

Figure S1. (a) XRD pattern and (b) EDS analysis of the product prepared by the hydrothermal route using NF and $(NH_4)_2HPO_4$ as the initial reactants.

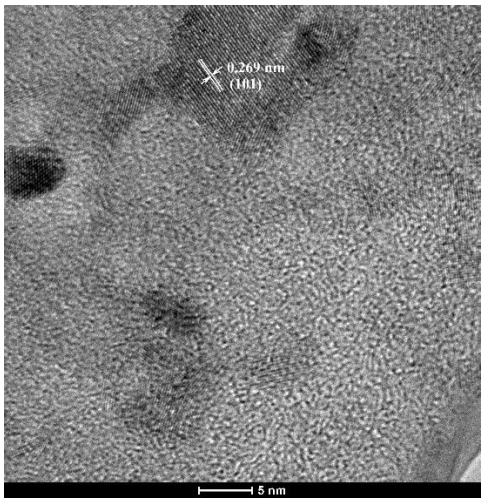

Figure S2. HRTEM image of FeNi LDH nanosheets.

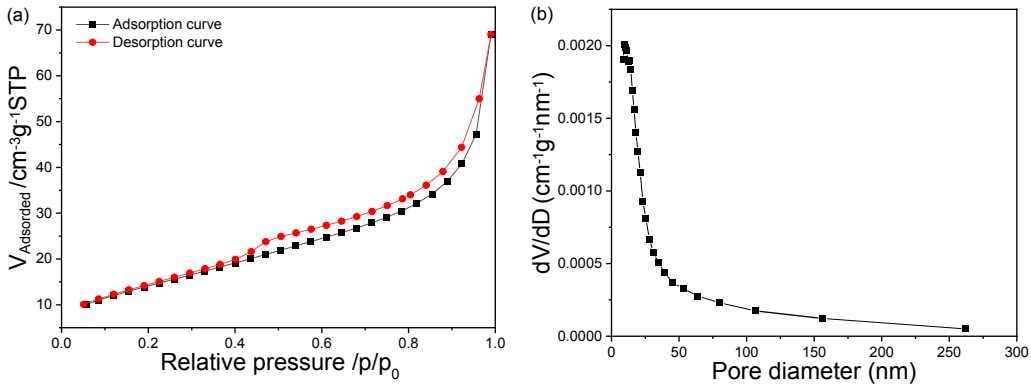

Figure S3. (a) N_2 adsorption-desorption isotherms and (b) pore diameter distribution of the as-obtained CFN@VSB-5 catalyst.

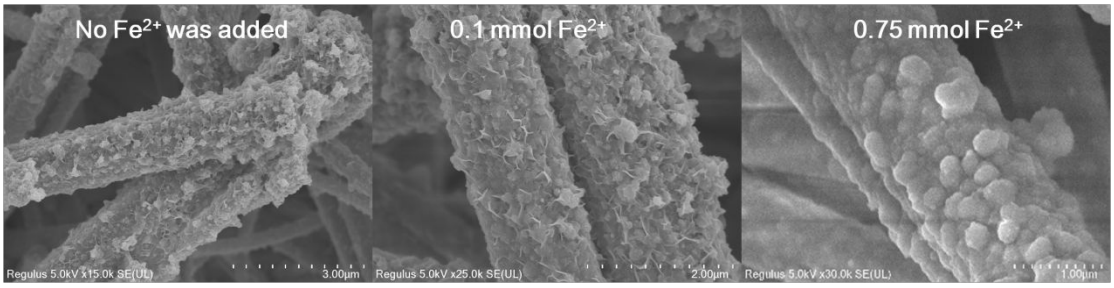

Figure S4. FESEM images of the catalysts deposited from the electrolytes with the initial Fe^{2+} ion amounts of 0, 0.1 and 0.75 mmol, respectively.

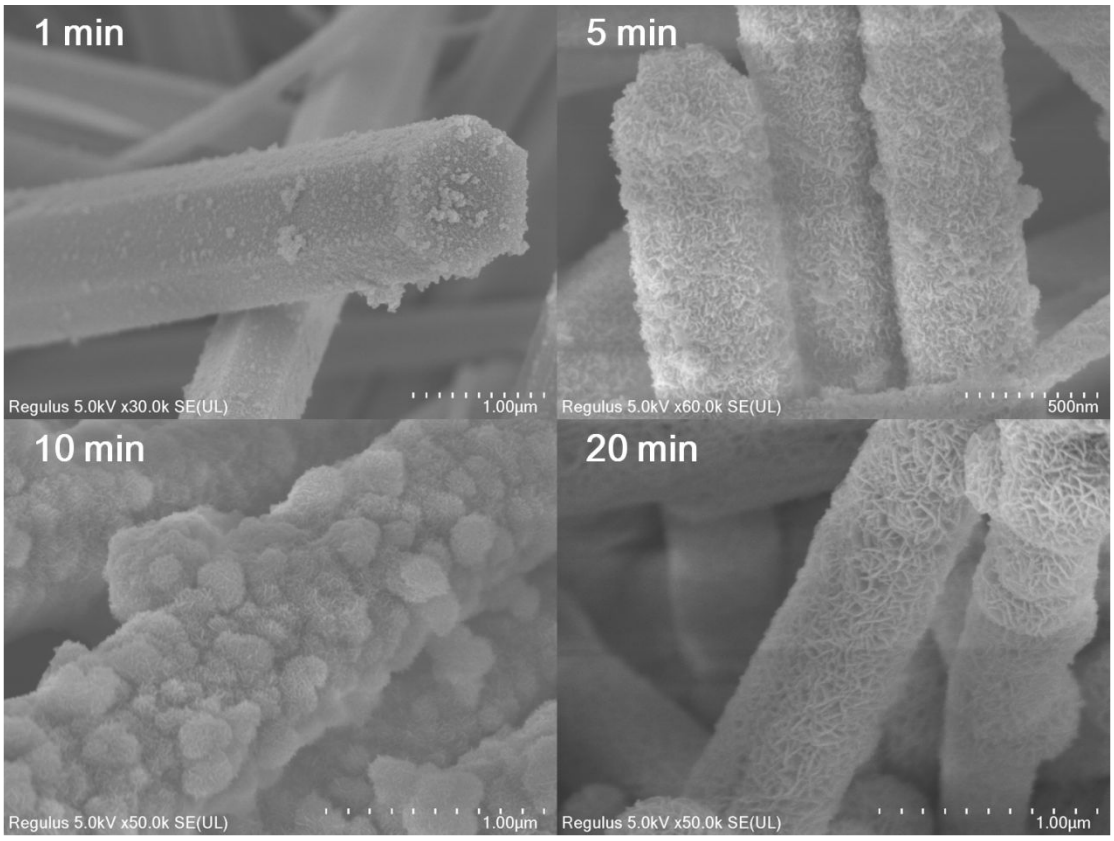

Figure S5. FESEM images of the catalysts deposited in the same conditions for various deposition durations.

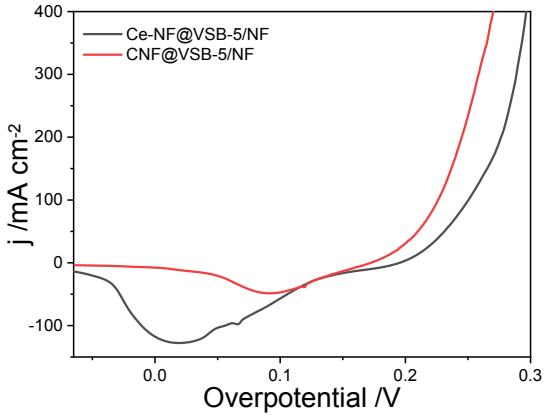

Figure S6. LSV curves of Ce-FN@VSB-5/NF prepared by two-step electrodeposition and CFN@VSB-5/NF prepared by one-step electrodeposition.

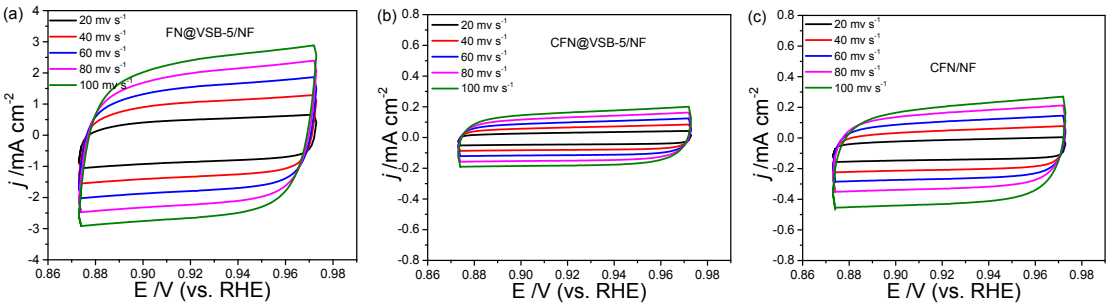

Figure S7. CV curves of FN@VSB-5/NF (a), and CFN@VSB-5/NF (b) and CFN/NF (c)

electrodes in non-faradic region at the scan rates of 20, 40, 60, 80 and 100 mV s^{-1}.

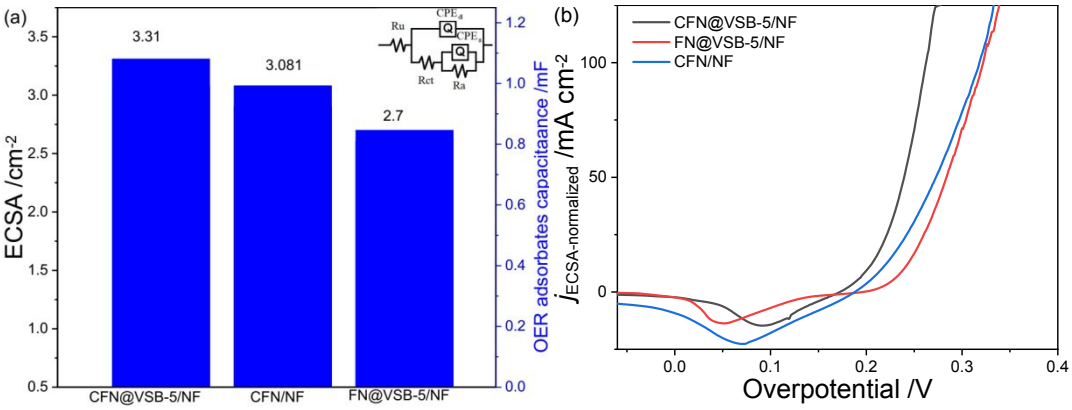

Figure S8. (a) the ECSA values of the CFN@VSB-5/NF, CFN/NF and FN@VSB-5/NF electrodes calculated according to the EIS method, and (b) the corresponding ECSA normalized LSV curves.

To estimate the ECSA through the EIS method, the capacitance of the adsorbed OER intermediates (labeled as C_a) was first calculated by EIS at 1.436 V (vs RHE). Then, the ECSA was calculated by C_a/C_s (C_s equals 0.3 mF cm^{-2}, stands for the specific area capacitance of a smooth $Ni(OH)_2$ surface.). Here, the inset shown in Fig.S8a was the equivalent circuit used to fit the impedance data. The indexes of the resistances R and the constant phase elements CPE stand for: u: uncompensated, ct: charge transfer (Faradaic process), dl: double layer and a: adsorbates (OER intermediates).

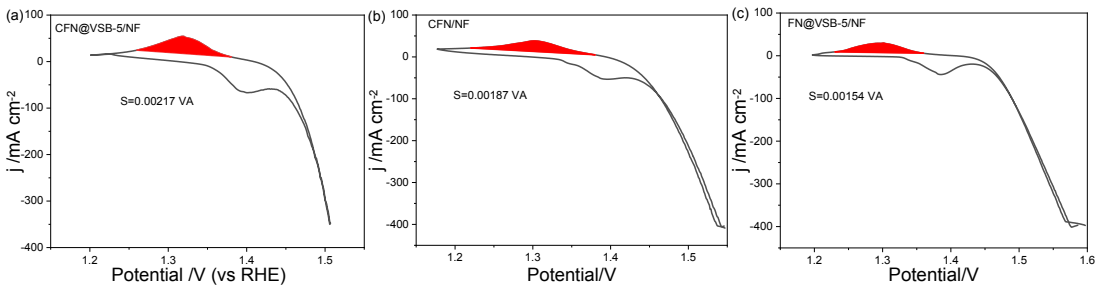

Figure S9. CV curves of the CFN@VSB-5/NF, CFN/NF and FN@VSB-5/NF electrodes at the scan rate of 1 mV s^{-1}.

Calculation of the active site number:

The number of the active sites involved in OER was determined based on the redox peak method.[1] Because the oxidation peak area equals the reduction peak one, the backward reduction peak was selected for calculating the number of active sites here. The CV curve was recorded at the scan rate of 1 mV s^{-1}. The number of active sites (τ) was calculated by the below equation:

$$\tau = S/(V \times q)$$

Where S (V · A) is integral area from CV reduction peak and the V is the scan rate (= 1 mV s^{-1}), q is 1.602×10^{-19} C (the charge of a single electron).

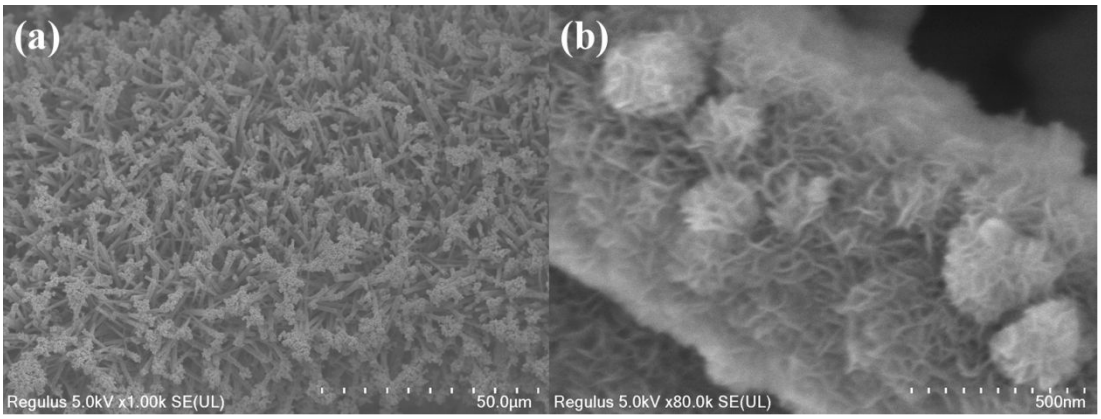

Figure S10. (a) Low- and (b) high-magnification FESEM images of the as-constructed CFN@VSB-5/NF electrode after OER test for 90 h at 20 mA cm^{-2}.

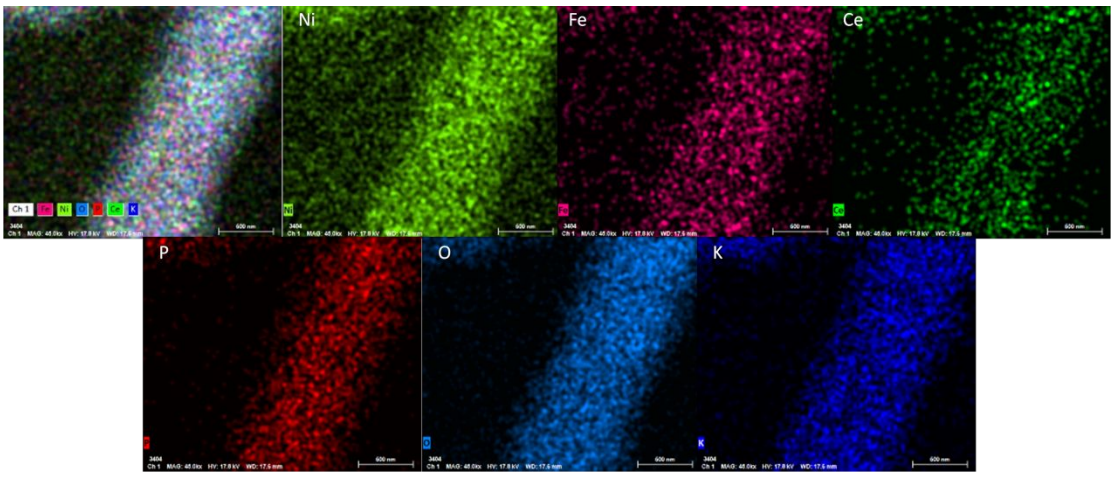

Figure S11. EDS-mapping images of the as-constructed CFN@VSB-5/NF electrode after OER test for 90 h at 20 mA cm^{-2}.

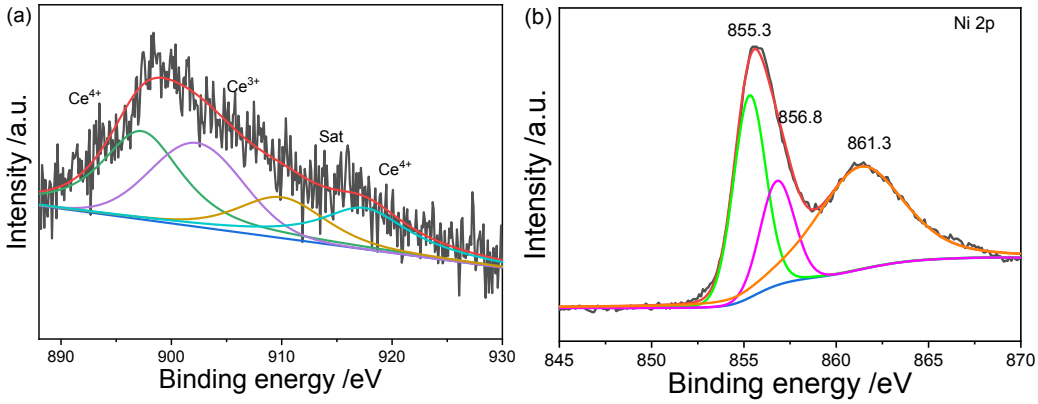

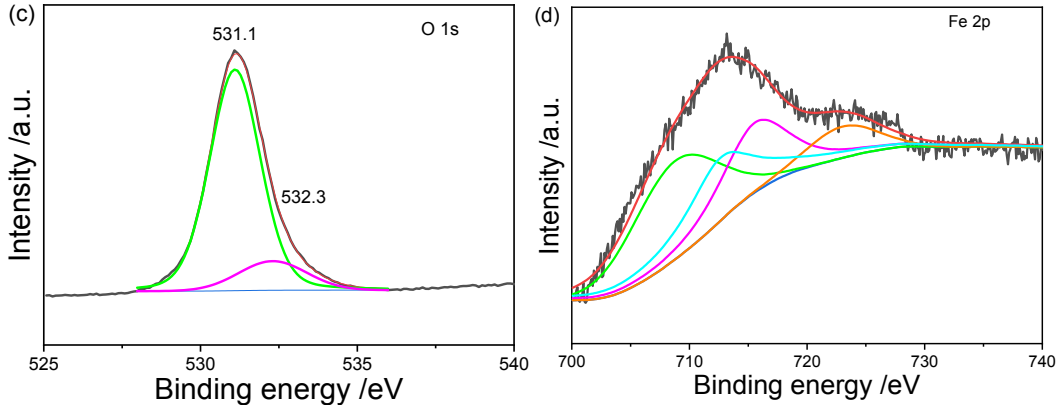

Figure S12. XPS spectra of various elements after OER test for 90 h at 20 mA cm^{-2}: (a) Ce 3d, (b) Ni 2p, (c) O 1s, and (d) Fe 2p.

Table S1. Comparison of the OER performances of the as-constructed CFN@VSB-5 catalyst with some reported catalysts.

Catalysts	Current density (mA cm^{-2})	Overpotential (mV)	Tafel slope (mV dec^{-1})	Ref.
NiCe@NiFe/NF-N	100	η_{100}=254	59.9	2
Fe-CoNi-OH	10	η_{10}=210	28.0	3
	100	η_{100}=248		
NiFe LDH-Ni(III)Li	10	η_{10}=248	35.0	4
Fe-Ni_5P_4/NiFeOH-350	10	η_{10}=221	35.0	5
U-Fe-β-$Ni(OH)_2$/NF-2	10	η_{10}=218	46.6	6
IrNi-$FeNi_3$/NF	20	η_{20}=240	36.01	7
Ni–Fe LDH DSNCs	20	η_{20}=246	71.0	8
P-V-NiFe LDH NSA	100	η_{100}=295	56.0	9
NFV NS-4h	100	η_{100}=280	65.0	10
CoCeNiFeZnCuOx	10	η_{10}=211	21.0	11
	100	η_{100}=307		
CFN@VSB-5/NF	10	η_{10}=185	43.1	This work
	50	η_{50}=210		
	100	η_{100}=226		

References:

(1) Anantharaj, S.; Ede, S. R.; Karthick, K.; Sankar, S. S.; Sangeetha, K, Karthik, P. E.; Kundu, S. Precision and correctness in the evaluation of electrocatalytic water splitting: revisiting activity parameters with a critical assessment, Energy Environ. Sci., 2018, 744-771.

(2) Liu, G.; Wang, M.; Wu, Y.; Li, N.; Zhao, F.; Zhao, Q.; Li, J. 3D porous network

heterostructure NiCe@NiFe electrocatalyst for efficient oxygen evolution reaction at large current densities, *Appl. Catal. B: Environ*. 2020, 260, 118199.

(3) Huang, C.; Zhong, Y.; Chen, J.; Li, J.; Zhang, W.; Zhou, J.; Zhang, Y.; Yu, L.; Yu, Y. Fe induced nanostructure reorganization and electronic structure modulation over CoNi (oxy)hydroxide nanorod arrays for boosting oxygen evolution reaction, *Chem. Eng. J.* 2021, 403, 126304.

(4) Xu, Z.; Ying, Y.; Zhang, G.; Li, K.; Liu, Y.; Fu, N.; Guo, X.; Yu, F.; Huang, H. Engineering NiFe layered double hydroxide by valence cont rol and intermediate stabilization toward the oxygen evolution reaction, *J. Mater. Chem. A*, 2020, 8, 26130-26138.

(5) Li, C.F.; Zhao, J.W.; Xie, L.J.; Wu, J.Q.; Li, G.R. Fe doping and oxygen vacancy modulated Fe-Ni_5P_4/NiFeOH nanosheets as bifunctional electrocatalysts for efficient overall water splitting, *Appl. Catal. B: Environ*. 2021, 291, 119987.

(6) Qiao, X.; Kang, H.; Li, Y.; Cui, K.; Jia, X.; Liu, H.; Qin, W.; Pupucevski, M.; Wu, G. Porous Fe-Doped beta-$Ni(OH)_2$ Nanopyramid Array Electrodes for Water Splitting, *ACS Appl. Mater. Interfaces,* 2020, 12, 36208-36219.

(7) Wang, Y.M.; Qian, G.F.; Xu, Q.L.; Zhang, H.; Shen, F.; Luo, L.; Yin, S.B. Industrially promising IrNi-$FeNi_3$ hybrid nanosheets for overall water splitting catalysis at large current density, *Appl. Catal. B: Environ*. 2021, 286, 119881.

(8) Zhang, J.; Yu, L.; Chen, Y.; Lu, X.F.; Gao, S.; Lou, X.W.D. Designed Formation of Double-Shelled Ni-Fe Layered-Double-Hydroxide Nanocages for Efficient Oxygen Evolution Reaction, *Adv. Mater*. 2020, 32, 1906432.

(9) Tang, Y.H.; Liu, Q.; Dong, L.; Wu, H.B.; Yu, X.Y. Activating the hydrogen evolution and overall water splitting performanceof NiFe LDH by cation doping and plasma reduction, *Appl. Catal. B: Environ*. 2020, 266, 118627.

(10) Tang, J.; Jiang, X.; Tang, L.; Li, Y.; Zheng, Q.; Huo, Y.; Lin, D. Ultrathin vanadium hydroxide nanosheets assembled on the surface of Ni–Fe-layered hydroxides as hierarchical catalysts for the oxygen evolution reaction, *Dalton Trans*. 2021, 50, 1053-1059.

(11) Huang, W.; Zhang, J.; Liu, D.; Xu, W.; Wang, Y.; Yao, J.; Tan, H.T.; Dinh, K.N.; Wu, C.; Kuang, M.; Fang, W.; Dangol, R.; Song, L.; Zhou, K.; Liu, C.; Xu, J.W.; Liu, B.; Yan, Q. Tuning the Electronic Structures of Multimetal Oxide Nanoplates to Realize Favorable Adsorption Energies of Oxygenated Intermediates, *ACS Nano*, 2020, 14, 17640-17651.